Effects of pressure work on natural convection flow around a sphere with radiation heat loss

T. Akhter[1]**, M.A. Alim**[2]

[1]Department of Mathematics, The University of Asia Pacific
Dhaka-1209, Bangladesh

[2]Department of Mathematics, Bangladesh University of Engineering and Technology
Dhaka-1000, Bangladesh
maalim@math.buet.ac.bd

Received: 2009-06-20 **Revised:** 2010-05-27 **Published online:** 2010-09-17

Abstract. The effects of pressure work with radiation heat loss on natural convection flow on a sphere have been investigated in this paper. The governing boundary layer equations are first transformed into a non-dimensional form and the resulting nonlinear partial differential equations are then solved numerically using finite-difference method with Keller-box scheme. We have focused our attention on the evaluation of shear stress in terms of local skin friction and rate of heat transfer in terms of local Nusselt number, velocity as well as temperature profiles. Numerical results have been shown graphically and tabular form for some selected values of parameters set consisting of radiation parameter Rd, pressure work parameter Ge, surface temperature parameter θ_w and the Prandtl number Pr.

Keywords: thermal radiation, Prandtl number, natural convection, pressure work.

Nomenclature

a	radius of the sphere [m]
C_f	skin-friction coefficient
C_p	specific heat at constant pressure [J kg^{-1}K^{-1}]
f	dimensionless stream function
g	acceleration due to gravity [m s^{-2}]
Ge	pressure work parameter
Gr	Grashof number
k	thermal conductivity [w m^{-1}K^{-1}]
Nu	Nusselt number
Pr	Prandtl number
q_r	radiative heat flux [W/m^2]
q_c	conduction heat flux [W/m^2]
Rd	radiation parameter
r	distance from the symmetric axis to the surface [m]
T	temperature of the fluid in the boundary layer [K]
T_∞	temperature of the ambient fluid [K]
T_w	temperature at the surface [K]
U	velocity component along the surface [m s^{-1}]
V	velocity component normal to the surface [m s^{-1}]
u	dimensionless velocity along the surface

v	dimensionless velocity normal to the surface	X	coordinate along the surface [m]
		Y	coordinate normal to the surface [m]

Greek symbols

α_r	Rosseland mean absorption coefficient [cm^3/s]	ν	kinematic viscosity $[\mathrm{m}^2/\mathrm{s}]$
		ξ	dimensionles coordinates
β	volumetric coefficient of thermal expansion [K^{-1}]	ρ	density of the fluid [kg m^{-3}]
		σ	Stephan–Boltzmann constant [J s^{-1}m^{-2}K^{-4}]
η	dimensionless coordinates		
θ	dimensionless temperature	σ_s	scattering coefficient [m^{-1}]
μ	dynamic viscosity of the fluid [kg m^{-1}s^{-1}]	τ_w	wall-shear-stress $[\mathrm{N}/\mathrm{m}^2]$
		ψ	stream function [m^{2}s^{-1}]

1 Introduction

Radiative energy passes perfectly through a vacuum thus radiation is significant mode of heat transfer when no medium is present. Radiation contributes substantially to energy transfer in furnaces, combustion chambers, fires, and to the energy emission from a nuclear explosion. Radiation must be considered in calculating thermal effects in rocket nozzles, power plants, engines, and high temperature heat exchangers. Radiation can sometimes be important even though the temperature level is not elevated and other modes of heat transfer are present. Radiation has a great effect in the energy equation which leads to a highly non-linear partial differential equation. Free convection flow is often encountered in cooling of nuclear reactors or in the study of the structure of stars and planets. The study of temperature and heat transfer has great importance in practical fields because of its almost universal occurrence in many branches of science and engineering. Again heat transfer analysis is most important for the proper sizing of fuel elements in the nuclear reactors cores to prevent burnout. The pressure work effect plays an important role in natural convection in various devices which are subjected to large deceleration or which operate at high rotational speeds and also in strong gravitational field processes on large scales (on large planets) and in geological processes. The discussion and analysis of natural convection flows, pressure work and radiation effects are generally ignored but here we have considered both these effects around a sphere. It is established that pressure work effects are generally rather more important both for gases and liquids. Also the problems of various types of shapes over or on a free convection boundary layer flow have been studied by many researchers.

Amongst them Nazar et al. [1], Huang and Chen [2] considered the free convection boundary layer on an isothermal sphere and on an isothermal horizontal circular cylinder both in a micropolar fluid. Molla et al. [3] have studied the problem of natural convection flow along a vertical wavy surface with uniform surface temperature in presence of heat generation or absorption. Again Alim et al. [4, 5] considered the pressure work effect along a circular cone and stress work effects on MHD natural convection flow along a sphere. Alam et al. [6–8] considered the pressure work effects for flow along vertical permeable circular cone, vertical flat plate and along a sphere. But they were not concerned about the radiation effects. They considered only viscous dissipation and pressure work effects.

Soundalgekar et al. [9] have studied radiation effects on free convection flow of a gas past a semi-infinite flat plate using the Cogley–Vincenti–Giles equilibrium model Cogley et al. [10], later Hossain and Takhar [11] have analyzed the effects of radiation using the Rosseland diffusion approximation which leads to non-similar solutions for free convection flow past a heated vertical plate. Akhter and Alim [12] studied the effects of radiation on natural convection flow around a sphere with uniform surface heat flux.

In the present work, the effects of pressure work with radiation heat loss on natural convection flow around a sphere have been investigated. The results are obtained for different values of relevant physical parameters. The natural convection boundary layer flow on a sphere of viscous incompressible fluid has been considered. The governing partial differential equations are reduced to locally non-similar partial differential forms by adopting appropriate transformations. The transformed boundary layer equations are solved numerically using implicit finite difference method together with Keller box scheme describe by Keller [13] and later by Cebeci and Bradshaw [14].

Numerical results have been shown in terms of local skin friction, rate of heat transfer, velocity profiles as well as temperature profiles for a selection of relevant physical parameters consisting of heat radiation parameter Rd, Prandtl number Pr and the pressure work parameter Ge are shown graphically. Some results for skin friction coefficient and the rate of heat transfer for different values of radiation parameter, pressure work parameter and the Prandtl number has been presented in tabular form as well.

2 Formulation of the problem

It is assumed that the surface temperature of the sphere is T_w, where $T_w > T_\infty$. Here T_∞ is the ambient temperature of the fluid, T is the temperature of the fluid in the boundary layer, g is the acceleration due to gravity, $r(x)$ is the radial distance from the symmetrical axis to the surface of the sphere and (u, v) are velocity components along the (x, y) axis.

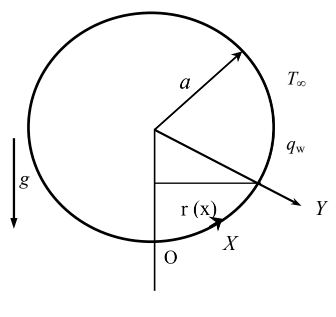

Fig. 1. Physical model and coordinate system.

Under the usual Bousinesq approximation, the equations those govern the flow are

$$\frac{\partial}{\partial X}(rU) + \frac{\partial}{\partial Y}(rV) = 0, \tag{1}$$

$$U\frac{\partial U}{\partial X} + V\frac{\partial U}{\partial Y} = \nu\frac{\partial^2 U}{\partial Y^2} + \rho g\beta(T - T_\infty)\sin\left(\frac{X}{a}\right), \tag{2}$$

$$U\frac{\partial T}{\partial X} + V\frac{\partial T}{\partial Y} = \frac{k}{\rho C_p}\frac{\partial^2 T}{\partial Y^2} - \frac{1}{\rho C_p}\frac{\partial q_r}{\partial Y} + \frac{T\beta}{\rho c_p}U\frac{\partial p}{\partial X}. \tag{3}$$

We know for hydrostatic pressure, $\partial p/\partial X = \rho g$.

The boundary conditions of equation (1) to (3) are

$$\begin{aligned} &U = V = 0, \quad T = T_w \quad \text{at } Y = 0, \\ &U \to 0, \qquad T \to T_\infty \quad \text{as } Y \to \infty, \end{aligned} \tag{4}$$

where ρ is the density, k is the thermal conductivity, β is the coefficient of thermal expansion, μ is the viscosity of the fluid, C_p is the specific heat due to constant pressure and q_r is the radiative heat flux in the y direction. In order to reduce the complexity of the problem and to provide a means of comparison with future studies that will employ a more detail representation for the radiative heat flux; we will consider the optically dense radiation limit. Thus the Rosseland diffusion approximation proposed by Siegel and Howell [15] and is given by simplified radiation heat flux term as:

$$q_r = -\frac{4\sigma}{3(\alpha_r + \sigma_s)}\frac{\partial T^4}{\partial Y}. \tag{5}$$

We now introduce the following non-dimensional variables:

$$\begin{aligned} &\xi = \frac{X}{a}, \quad \eta = Gr^{1/4}\left(\frac{Y}{a}\right), \\ &u = \frac{a}{\nu}Gr^{-1/2}U, \quad v = \frac{a}{\nu}Gr^{-1/4}V, \\ &\theta = \frac{T - T_\infty}{T_w - T_\infty}, \quad Gr = g\beta(T_w - T_\infty)\frac{a^3}{\nu^2}, \end{aligned} \tag{6}$$

where ν ($= \mu/\rho$) is the reference kinematic viscosity and Gr is the Grashof number, θ is the non-dimensional temperature function.

Substituting variable (6) into equations (1)–(3) leads to the following non-dimensional equations

$$\frac{\partial}{\partial \xi}(ru) + \frac{\partial}{\partial \eta}(rv) = 0, \tag{7}$$

$$u\frac{\partial u}{\partial \xi} + v\frac{\partial u}{\partial \eta} = \frac{\partial^2 u}{\partial \eta^2} + \theta\sin\xi, \tag{8}$$

$$u\frac{\partial \theta}{\partial \xi} + v\frac{\partial \theta}{\partial \eta} = \frac{1}{Pr}\frac{\partial}{\partial \eta}\left[\left\{1+\frac{4}{3}Rd(1+\Delta\theta)^3\right\}\frac{\partial \theta}{\partial \eta}\right] + Ge\left(\theta+\frac{T_\infty}{T_w - T_\infty}\right)u, \tag{9}$$

where $\Delta = \frac{T_w}{T_\infty} - 1$ with the boundary conditions (4) as

$$\begin{aligned} &u = v = 0, \quad \theta = 1 \quad \text{at } \eta = 0, \\ &u \to 0, \qquad \theta \to 0 \quad \text{as } \eta \to \infty, \end{aligned} \tag{10}$$

where Rd is the radiation-conduction parameter, Pr is the Prandtl number and Ge is the pressure work parameter defined respectively as

$$Rd = \frac{4\sigma T_\infty^3}{k(\alpha_r + \sigma_s)}, \quad Pr = \frac{\mu C_p}{k} \quad \text{and} \quad Ge = \frac{g\beta a}{C_P}. \tag{11}$$

To solve equations (8)–(9), subject to the boundary conditions (10), we assume the following variables

$$\psi = \xi r(\xi) f(\xi, \eta), \quad \theta = \theta(\xi, \eta), \tag{12}$$

where ψ is the non-dimensional stream function defined in the usual way as

$$u = \frac{1}{r}\frac{\partial \psi}{\partial \eta} \quad \text{and} \quad v = -\frac{1}{r}\frac{\partial \psi}{\partial \xi}. \tag{13}$$

Substituting (13) into equations (8)–(9), after some algebra the transformed equations take the following form

$$\begin{aligned} &\frac{\partial^3 f}{\partial \eta^3} + \left(1 + \frac{\xi}{\sin \xi}\cos \xi\right) f \frac{\partial^2 f}{\partial \eta^2} - \left(\frac{\partial f}{\partial \eta}\right)^2 + \frac{\sin \xi}{\xi}\theta \\ &\quad = \xi\left(\frac{\partial f}{\partial \eta}\frac{\partial^2 f}{\partial \xi \partial \eta} - \frac{\partial f}{\partial \xi}\frac{\partial^2 f}{\partial \eta^2}\right), \end{aligned} \tag{14}$$

$$\begin{aligned} &\frac{1}{Pr}\frac{\partial}{\partial \eta}\left[\left\{1 + \frac{4}{3}Rd(1 + \Delta\theta)^3\right\}\frac{\partial \theta}{\partial \eta}\right] + \left(1 + \frac{\xi}{\sin \xi}\cos \xi\right) f \frac{\partial \theta}{\partial \eta} \\ &\quad + Ge\left(\theta + \frac{T_\infty}{T_w - T_\infty}\right)\xi f' = \xi\left(\frac{\partial f}{\partial \eta}\frac{\partial \theta}{\partial \xi} - \frac{\partial \theta}{\partial \eta}\frac{\partial f}{\partial \xi}\right). \end{aligned} \tag{15}$$

Along with boundary conditions

$$\begin{aligned} f = \frac{\partial f}{\partial \eta} = 0, \quad \theta = 1 \quad \text{at } \eta = 0, \\ \frac{\partial f}{\partial \eta} \to 0, \quad \theta \to 0 \quad \text{as } \eta \to \infty. \end{aligned} \tag{16}$$

It can be seen that near the lower stagnation point of the sphere, i.e., at $\xi = 0$, equations (14) and (15) reduce to the following ordinary differential equations:

$$f''' + 2ff'' - f'^2 + \theta = 0, \tag{17}$$

$$\frac{1}{\Pr}\left[\left\{1 + \frac{4}{3}Rd\left(1 + \Delta\theta\right)^3\right\}\theta'\right]' + 2f\theta' = 0. \tag{18}$$

Subject to the boundary conditions

$$
\begin{aligned}
f(0) = & f'(0) = 0, \quad \theta(0) = 1, \\
& f' \to 0, \qquad \theta \to 0 \qquad \text{as } \eta \to \infty.
\end{aligned} \tag{19}
$$

In the above equations primes denote the differentiation with respect to η.

In practical applications, the physical quantities of principle interest are the wall-shear-stress, the heat transfer rate in terms of the skin-friction coefficients C_f and Nusselt number Nu_x respectively, which can be written as

$$
C_f = \frac{Gr^{-3/4}a^2}{\rho\nu}\tau_w \quad \text{and} \quad Nu = \frac{a\,Gr^{-1/4}}{k(T_w - T_\infty)}q_w, \tag{20}
$$

where

$$
\tau_w = \mu\left(\frac{\partial u}{\partial y}\right)_{y=0} \quad \text{and} \quad q_w = -k\left(\frac{\partial T}{\partial y}\right)_{y=0}. \tag{21}
$$

Here we have used a reference velocity $U = \frac{\nu Gr^{1/5}}{a}$.

Using the variables (6) and (13) and the boundary condition (19) into (20)–(21), we get

$$
C_f = \xi f''(\xi, 0), \tag{22}
$$

$$
Nu = -\left(1 + \frac{4}{3}Rd\theta_w^3\right)\theta'(\xi, 0), \tag{23}
$$

where $\theta_w = T_w/T_\infty$.

The values of the velocity and temperature distribution are calculated respectively from the following relations:

$$
u = \frac{\partial f}{\partial \eta}, \quad \theta = \theta(\xi, \eta). \tag{24}
$$

3 Results and discussion

The present problem has been solved numerically for different values of relevant physical parameters and for a fixed value of $\Delta = 0.1$. Results have been obtained in terms of local skin friction and the rate of heat transfer in terms of local Nusselt number, velocity as well as temperature profiles.

Velocity and temperature profiles are shown in Figs. 2(a)–2(b) for different values of radiation parameter Rd while Prandtl number $Pr = 7.0$ and pressure work parameter $Ge = 1.5$. From Fig. 2(a) it is observed that for higher values of radiation the velocity becomes higher and there is no significant change found in the boundary layer thickness.

Fig. 2(b) shows that the temperature becomes higher from the wall value of temperature along η direction and reaches at maximum values which occur between $\eta = 0.5$ to

1.5, then all the profiles gradually decrease, cross each other near the point $\eta = 1.4$ and finally approach to zero, the asymptotic value.

Effects of the variation of pressure work on velocity and temperature profiles are shown in the Figs. 3(a) and 3(b). Significant changes have been found in maximum velocity and temperature due to the change of Ge. In Fig. 3(a) for $Ge = 0.1$ the maximum velocity is 0.19532 which occurs at $\eta = 0.88811$ and for $Ge = 2.5$ the maximum velocity is 0.77141 which occurs at $\eta = 0.78384$. Thus we observe that due to the change of Ge from 0.1 to 2.5 the velocity rises up 294.95 %. Again in Fig. 3(b) small value of Ge $(= 0.1)$ gives the typical temperature profile which is maximum temperature at wall then it gradually decrease along η direction and finally approaches to the asymptotic value (zero). But larger values of Ge do not show the typical temperature profiles. In this case along η direction temperature gradually increased from the wall value to the peak and then decrease and approach to the asymptotic value.

Moreover, in the Fig. 4(a) it is observed that the velocity decrease with increasing Pr. Fig. 4(b) shows that the temperature increase along η direction up to the maximum value and then gradually decreases to zero. All the temperature profiles cross each other near $\eta = 1.1$. Also for higher values of Pr temperature goes up near the wall but it cause the thermal boundary layer thickness to reduce and thus the temperature profiles have a crossing point near $\eta = 1.1$. The value of $\xi = 0.3927$ has been chosen to obtain all the results in Figs. 2, 3 and 4.

Fig. 5(a) shows the skin friction against ξ for different values of radiation parameter Rd. From this figure we observe that skin friction becomes lower for higher values of radiation. From Fig. 5(b) we see that the rate of heat transfer increase, between $\xi = 0.0$ to 0.1 intersect at $\xi = 0.1$ and then decrease for higher values of Rd within the region $\xi > 0.1$. In this figure we found both positive and negative Nusselt numbers. This is due to the variation of fluid temperature near the wall. The rate of heat transfer changes its sign in case of fluid temperature near the wall becomes higher or lower than the wall temperature which may occur due to the imposed conditions on the problem.

Fig. 6(a) shows the skin friction coefficient C_f for different values of pressure work parameter Ge. It is observed from the figure that the pressure work have great influence on skin friction as well as on the rate of heat transfer. Frictional force at the wall becomes much higher towards the downstream for higher values of Ge and the rate of heat transfer as shown in Fig. 6(b) gradually decreased for higher values of pressure work parameter.

Again from Figs. 7(a) and 7(b) it is observed that the Pr have similar type of influences on skin friction and on the rate of heat transfer but those are not as much as that of Ge, also rate of heat transfer increase between $\xi = 0.0$ to 0.7 intersect at $\xi = 0.7$ and then decrease for increasing Pr while $\xi > 0.7$.

Table 1 shows the numerical values of skin friction coefficient C_f and rate of heat transfer Nu at the surface of the sphere from $\xi = 0.0$ (lower stagnation point) to $\xi = \pi/2$ for different values of Ge. As in Figs. 6(a) and 6(b) the numerical data also shows that the frictional force at the wall becomes higher at the downstream and the rate of heat transfer gradually decreases for higher values of Ge.

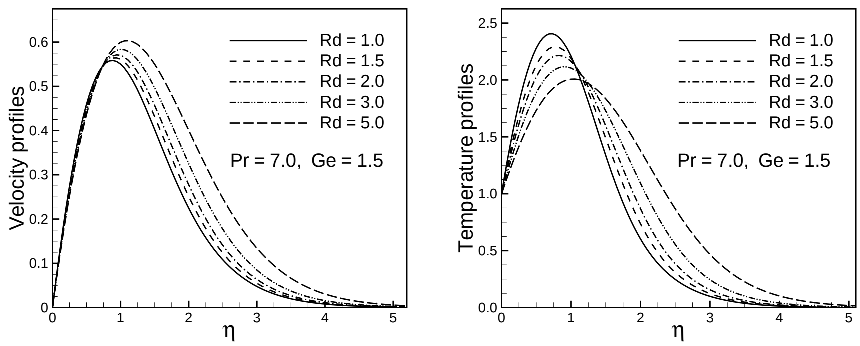

(a) (b)

Fig. 2. Velocity (a) and temperature (b) profiles for different values of Rd while $Pr = 7.0$ and $Ge = 1.5$.

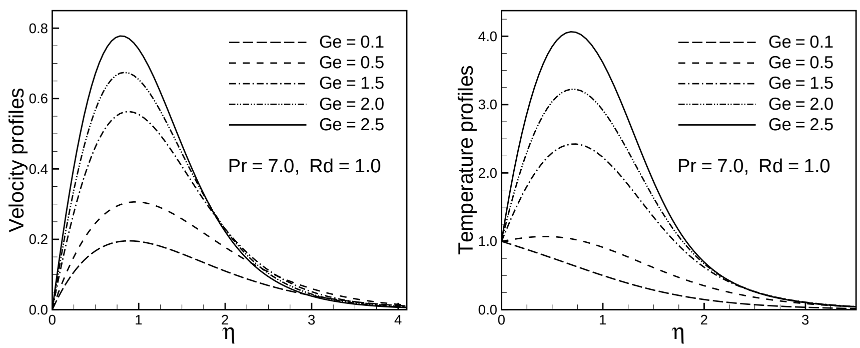

(a) (b)

Fig. 3. Velocity (a) and temperature (b) profiles for different values of Ge while $Rd = 1.0$ and $Pr = 7.0$.

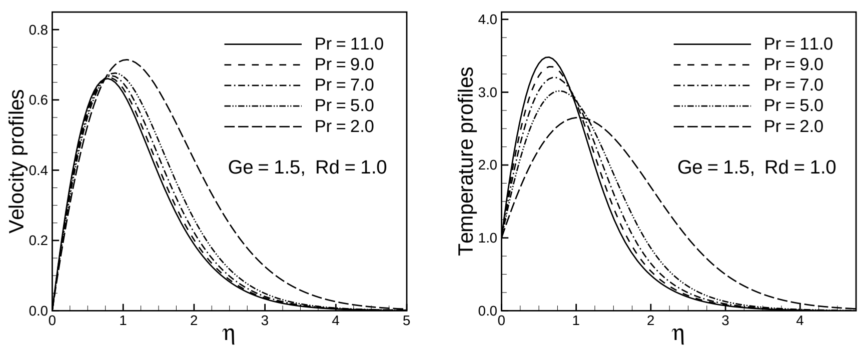

(a) (b)

Fig. 4. Velocity (a) and temperature (b) profiles for different values of Pr while $Ge = 1.5$ and $Rd = 1.0$.

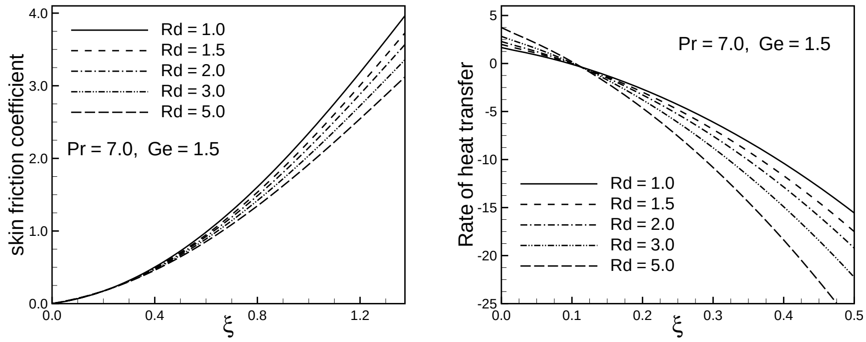

(a) (b)

Fig. 5. Skin friction (a) and heat transfer (b) coefficients for different values of Rd while $Pr = 7.0$ and $Ge = 1.5$.

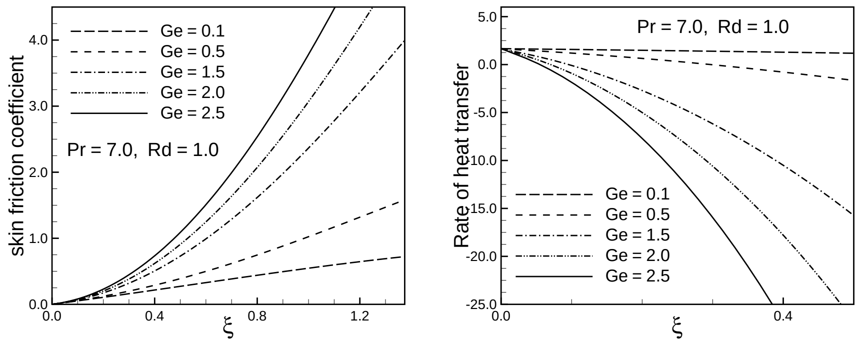

(a) (b)

Fig. 6. Skin friction (a) and heat transfer (b) coefficients for different values of Ge while $Rd = 1.0$ and $Pr = 7.0$.

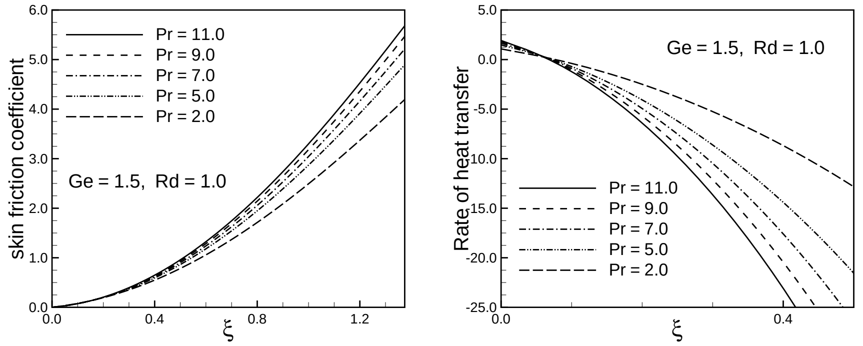

(a) (b)

Fig. 7. Skin friction (a) and heat transfer (b) coefficients for different values of Pr while $Rd = 1.0$ and $Ge = 1.5$.

Table 1. Skin friction coefficient and rate of heat transfer against ξ for different values of Ge against fixed radiation numbers $Rd = 1.0$ and $Pr = 0.72$.

	$Ge = 1.0$		$Ge = 0.8$	
ξ	C_f	Nu	C_f	Nu
0.00000	0.00000	0.723900	0.00000	0.723900
0.10472	0.07890	0.283260	0.07746	0.380840
0.20944	0.17176	−0.248780	0.16556	−0.018690
0.31416	0.27965	−0.886880	0.26493	−0.487330
0.40143	0.38118	−1.498300	0.35638	−0.929900
0.50615	0.51657	−2.327260	0.47612	−1.522890
0.61087	0.66594	−3.261580	0.60607	−2.183580
0.71558	0.82812	−4.304680	0.74523	−2.913080
0.80285	0.97200	−5.260890	0.86732	−3.575030
0.90757	1.15368	−6.519030	1.01995	−4.436790
1.01229	1.34342	−7.906760	1.17772	−5.375830
1.50098	2.26681	−16.51492	1.92379	−10.95695
1.57080	2.39328	−18.10731	2.02284	−11.94642
	$Ge = 0.4$		$Ge = 0.1$	
ξ	C_f	Nu	C_f	Nu
0.00000	0.00000	0.72390	0.00000	0.72390
0.10472	0.07470	0.56152	0.07277	0.64416
0.20944	0.15396	0.38736	0.14612	0.68446
0.31416	0.23755	0.19464	0.21947	0.60139
0.40143	0.31025	0.01984	0.28018	0.56370
0.50615	0.40074	−0.20692	0.35200	0.51620
0.61087	0.49417	−0.45213	0.42215	0.46614
0.71558	0.58984	−0.71575	0.49002	0.41351
0.80285	0.67067	−0.94951	0.54439	0.36768
0.90757	0.76820	−1.24698	0.60649	0.31033
1.01229	0.86535	−1.56305	0.66460	0.25042
1.50098	1.27877	−3.28790	0.86512	−0.06165
1.57080	1.32730	−3.56784	0.88200	−0.11017

4 Conclusion

Natural convection flow around a sphere has been studied with the effects of pressure work and radiation heat loss. From the present investigation the following conclusions may be drawn:

Significant effects of pressure work on velocity and temperature profiles as well as on skin friction and the rate of heat transfer have been found in this study. Due to the change of Ge the velocity rises up $294.95\,\%$. For larger values of Ge the temperature profiles change its typical nature, such as along η direction temperature gradually increased from the wall value to the peak and then decrease and approach to the asymptotic value.

Also the frictional force at the wall becomes much higher towards the downstream for higher values of Ge and the rate of heat transfer gradually decreased for higher values of pressure work parameter.

The velocity becomes higher for higher values of radiation and there is no significant change found in the boundary layer thickness. For higher values of radiation the maximum temperature decreases. Along the η direction temperature goes up from the wall value and reaches at maximum then gradually decrease and finally approach to zero. Maximum temperature occurs away from the wall which is not only the radiation effect but also the influence of pressure work as well. Also the skin friction becomes lower for higher values of radiation and rate of heat transfer increase near the wall and then decrease for higher values of Rd.

Prandtl number rise leads to decrease the velocity and temperature and increase the skin friction and reduce the rate of heat transfer.

References

1. R. Nazar, N. Amin, T. Grosan, I. Pop, Free convection boundary layer on an isothermal sphere in a micropolar fluid, *Int. Commun. Heat Mass*, **29**(3), pp. 377–386, 2002.

2. M.J. Huang, C.K. Chen, Laminar free convection from a sphere with blowing and suction, *J.Heat Transf.*, **109**, pp. 529–532, 1987.

3. Md.M. Molla, M.A. Taher, Md.M.K. Chowdhury, Md.A. Hossain, Magnetohydrodynamic natural convection flow on a sphere in presence of heat generation, *Nonlinear Anal. Model. Control*, **10**(4), pp. 349–363, 2005.

4. M.A. Alim, Md.M. Alam, Md.M.K. Chowdhury, Pressure work effect on natural convection flow from a vertical circular cone with suction and non-uniform surface temperature, *Journal of Mechanical Engineering*, The Institution of Engineers, Bangladesh, **36**, pp. 6–11, 2006.

5. M.A. Alim, Md.M. Alam, Md.M.K. Chowdhury, Work stress effects on mhd natural convection flow along a sphere, *Thammasat Int. J. Sci. Tech.*,**13**(1), pp. 1–10, 2008.

6. Md.M. Alam, M.A. Alim, Md.M.K. Chowdhury, Free convection from a vertical permeable circular cone with pressure work and non-uniform surface temperature, *Nonlinear Anal. Model. Control*, **12**(1), pp. 21–32, 2007.

7. Md.M. Alam, M.A. Alim, Md.M.K. Chowdhury, Effect of pressure stress work and viscous dissipation in natural convection flow along a vertical flat plate with heat conduction, *Journal of Naval Architecture and Marine Engineering*, **3**(2), pp. 69–76, 2006.

8. Md.M. Alam, M.A. Alim, Md.M.K. Chowdhury, Viscous dissipation effects with MHD natural convection flow on a sphere in presence of heat generation, *Nonlinear Anal. Model. Control*, **12**(4), pp. 447–459, 2007.

9. V.M. Soundalgekar, H.S. Takhar, N.V. Vighnesam, The combined free and forced convection flow past a semi-infinite vertical plate with variable surface temperature, *Nucl. Eng. Des.*, **110**, pp. 95–98, 1960.

10. A.C. Cogley, W.G. Vincenti, S.E. Giles, Differential approximation for radiation transfer in a nongray near equilibrium, *AIAA J.*, **6**, pp. 551–553, 1968.

11. M.A. Hossain, H.S. Takhar, Radiation effect on mixed convection along a vertical plate with uniform surface temperature, *Heat Mass Transfer*, **31**, pp. 243–248, 1996.

12. Tahmina Akhter, M.A. Alim, Effects of radiation on natural convection flow around a sphere with uniform surface heat flux, *Journal of Mechanical Engineering*, The Institution of Engineers, Bangladesh, **39**(1), pp. 50–56, 2008.

13. H.B. Keller, Numerical methods in boundary layer theory, *Annu. Rev. Fluid Mech.*, **10**, pp. 417–433, 1978.

14. T. Cebeci, P. Bradshaw, *Physical and Computational Aspects of Convective Heat Transfer*, Springer, New York, 1984.

15. R. Siegel, J. R. Howell, *Thermal Radiation Heat Transfer*, McGraw-Hill, New York, 1972.